ELSEVIER

Journal of Nuclear Materials 290–293 (2001) 1013–1017

journal of nuclear materials

www.elsevier.nl/locate/jnucmat

Gas puff fueled H-mode discharges with good energy confinement above the Greenwald density limit on DIII-D ☆

T.H. Osborne [a,*], M.A. Mahdavi [a], M. Chu [a], M.E. Fenstermacher [a,b], R. La Haye [a], A.W. Leonard [a], G. McKee [a,c], T.W. Petrie [a], C. Rettig [a,d], M. Wade [a,e], J. Watkins [a,f], DIII-D Team

[a] *General Atomics, 13-412, P.O. Box 85608, San Diego, CA 92138-9784 USA*
[b] *Lawrence Livermore National Laboratory, USA*
[c] *University of Wisconsin-Madison, USA*
[d] *University of California-Los Angeles, USA*
[e] *Oak Ridge National Laboratory, USA*
[f] *Sandia National Laboratory, USA*

Abstract

Tokamak discharges with electron densities as high as 1.4 times the Greenwald density, and good energy confinement, $H_{ITER89P} = 1.9$, were obtained with D_2 gas puffing on DIII-D. The divertor configuration of these discharges, low triangularity with pumping of the private flux region, was important in avoiding a transition to the L-mode or Type III ELM regimes in which energy confinement was reduced. Although these discharges show a decrease in H-mode pedestal energy at high density through reduction in the edge pressure gradient, peaking of the density profile compensated for the effect of this decrease on the overall stored energy. Spontaneous density profile peaking occurred under conditions which enhance the neoclassical Ware pinch. The high density phase was terminated by an internal MHD event that has the characteristics of a neoclassical tearing mode.

Keywords: Density limit; DIII-D; Edge plasma

1. Introduction

Achieving ignition or high $Q = P_{FUSION}/P_{AUX}$ in a Tokamak reactor requires high energy confinement at high density [1]. This requirement is the result of the fact that $P_{FUSION} \propto n^2$ while $P_{LOSS} \propto n^2/H^2$, where H is the energy confinement enhancement factor over H-mode scaling, so that $P_{FUSION}/P_{LOSS} \propto H^2$. High H however implicitly assumes H-mode confinement, which requires $P_{LOSS} \geqslant P_{LH}$, where P_{LH} is the L- to H-mode transition power. Since $P_{LH} \propto n$ [2], there is a minimum density required for the fusion power to sustain H-mode.

Because of the large size, high temperatures, and high densities required in reactors, direct particle fueling of the plasma core, as with neutral beams or pellets, is difficult and fueling via an edge particle source, such as gas puffing, may still be required. Gas puff fueling of H-mode plasmas usually leads to loss of energy confinement when the electron density, n_e, approaches the Greenwald density, $n_G(10^{20}\ m^{-3}) = I_P(MA)/[\pi a^2\ (m)]$ [3,4], typically beginning in the range $0.7 < n_e/n_G < 1.0$. The causes of confinement loss at high density in DIII-D are discussed in Section 2.

In DIII-D, D_2 gas puff fueled discharges were obtained with n_e/n_G as high as 1.4, with confinement enhancement relative to L-mode scaling, $H_{ITER89P} = 1.9$ (Fig. 1). The discharges described in this article were in a single null divertor configuration with the ∇B drift

☆ Work supported by US DOE under Contract Nos. DE-AC03-99ER54463, DE-AC04-94AL85000, and W-7405-ENG-48.

* Corresponding author. Tel.: +1-619 455 3479; fax: +1-619 455 4156.

E-mail address: osborne@fusion.gat.com (T.H. Osborne).

0022-3115/01/$ - see front matter
PII: S0022-3115(00)00660-7

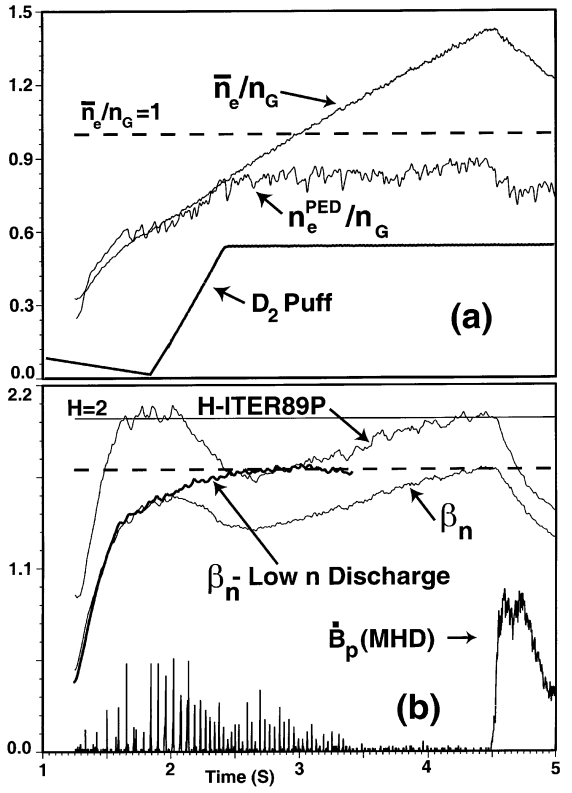

Fig. 1. High density gas puff fueled discharge with good energy confinement. (a) Line average density, $\bar{n}_e$, rises in response to gas puff, while H-mode pedestal density, n_e^{PED}, remains fixed. (b) Plasma stored energy $\propto \beta_n = \beta(\%)aB/I(\mathrm{MA})$, increases as density profile peaks. β_n reaches a level comparable with that of a low density discharge at the same heating power. Density rise is terminated by an MHD event (primarily $m = 3$, $n = 2$ mode).

towards the x-point, with $0.6 < I_P < 1.5$ MA and safety factor at the 95% flux surface, $2.8 < q_{95} < 4.2$. Heating power was by neutral beam injection at a moderate level, $1.5 < P_B < 7.5$ MW. In addition to the reactor relevant q value, normalized β, $\beta_N = \beta(\%)/I_P(\mathrm{MA})/a(m)B(T))$, values up to 1.9 were achieved at $n_e/n_G = 1.3$. Gas puff fueling was through a valve located in the upper outer region of the vessel wall well away from the divertor region. Gas puff rates up to 200 Tl/s were used with the valve typically being opened to the prescribed flow rate for the duration of the H-mode phase. The best performance was obtained in low triangularity discharges with pumping of the private flux region of the divertor. The effect of the divertor configuration and pumping on the performance at high density is discussed in Section 3. The confinement improvement with increasing density observed in the later stages of the highest density discharges was associated with spontaneous peaking of the density profile. This peaking of the density profile and its possible relation to the neoclassical Ware pinch is discussed in Section 4. The continuous rise of the density and energy confinement in the later phase of the highest density discharges was terminated by an internal MHD event, which will be discussed in Section 5. A summary and discussion is given in Section 6.

2. Causes of confinement reduction in high density H-mode discharges

Excluding discharges with internal transport barriers and ELM free VH-mode discharges, the highest energy confinement on DIII-D is achieved in discharges with Type I ELMs [5]. Since Type I ELMs limit the H-mode pedestal pressure, raising the pedestal density with gas puff fueling can reduce the pedestal temperature to the critical value for transition to Type III ELMs [6,7] or L-mode [7,8]. In DIII-D both discharges with Type III ELMs and L-mode are reduced in energy confinement relative to the Type I regime.

Similar to results on ASDEX-Upgrade [9], the temperature profiles in the high density regime on DIII-D are stiff [10], that is $T(\rho) \propto T^{PED}$ where T^{PED} is the temperature at the top of the H-mode pedestal. Given a stiff temperature profile, the stored energy, W, is proportional to the product of the H-mode pedestal pressure and an increasing function of the peaking factor for the density profile, $W \propto p^{PED} f(n^0/n^{PED})$. In this regime reduction in the plasma stored energy in response to the edge particle source can result from broadening of the density profile, or a reduction in the pedestal pressure. Both of these effects play a role in the initial drop in stored energy and H factor following the start of gas puffing shown in Fig. 1. The cause of the edge pressure reduction in response to gas puffing is primarily the result of a decrease in the pressure gradient before an ELM that begins in the range of $0.7 < n_e^{PED}/n_G < 0.8$ [10]. The scaling of the pressure reduction suggests that the low n, ideal, edge kink modes thought to be the cause of the ELM [11] become resistive [10]. In the later phase of the highest density discharges peaking of the density profile compensates for the reduction in pedestal pressure and the stored energy increases to match the low density value (Fig. 2(a)). Discharges under conditions that do not result in as strong a density peaking (discussed in Section 4) do not recover from the pedestal pressure loss and have reduced energy confinement (Fig. 2(b)).

3. Effect of divertor configuration

The highest pedestal and line average densities were obtained in discharges in which the divertor strike points were located at large major radius (Fig. 3). The main effect of the change in the divertor strike point location,

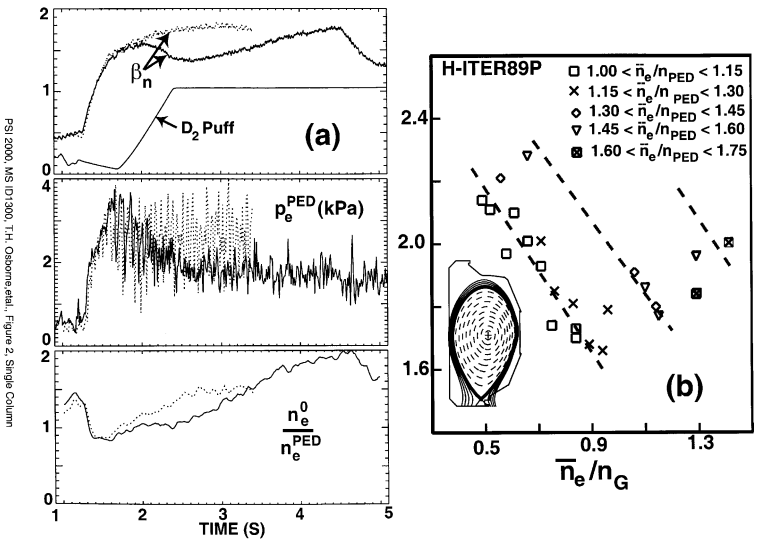

Fig. 2. (a) Normalized β, β_N, in high density discharge of Fig. 1 recovers from pedestal pressure, p_e^{PED}, loss through peaking of the density profile (n_e^0/n_e^{PED} is the ratio of axial to H-mode pedestal density) (solid curves). Low density discharge with no gas puffing during the H-mode phase (dotted curves) is shown for comparison. (b) Energy confinement enhancement factor relative to L-mode scaling, $H_{ITER89P}$ decreases at high density for fixed density peaking, but high confinement can be recovered at high density with higher density profile peaking.

R_{DS}, was through variation in the threshold temperature for the transition between the high confinement Type I ELM regime and the Type III or L-mode regimes. Since there was little change in the H-mode pedestal pressure over the range in strike point locations in this experiment, an increase in the threshold temperature for the onset of the degraded regimes resulted in a reduction in the pedestal density that could be achieved while maintaining high energy confinement. At large R_{DS} a transition occurred to Type III ELMs first and subsequently to L-mode with increasing gas puff rate. In contrast, at reduced R_{DS} the discharge went directly into L-mode, suggesting that the Type III ELM critical temperature was below the L-mode temperature (Fig. 3(a)). Thus the variation in pedestal density which could be achieved with Type I ELMs as a function of strike point radius was a composite of the variation of L-mode and Type III ELM critical temperatures (Fig. 3(b)). There was also an increase in the critical temperature for Type III and L-mode transition with increasing toroidal field as has been observed in other experiments [6,8] and predicted theoretically [7].

As part of the study of the effect of strike point location on highest density obtainable with high energy confinement, discharges were run with and without divertor pumping (see Fig. 3 for pump configuration). No significant difference was found in the Type III or L-mode critical temperatures with or without pumping, although the gas puff rates required to produce the transition were increased by a factor of 3 or more with pumping. Also discharges with divertor pumping were operationally easier to run reproducibly to high density.

4. Particle pinch and density peaking

As discussed in Section 2, high confinement at high density is associated with spontaneous peaking of the density profile. Typically the temperature profile and H-mode pedestal density reach steady state while the central density continues to rise. In many cases this rise in core density is nearly linear (Fig. 1) and is terminated only by onset of MHD instability. The density profile peaking is enhanced at low heating power (Fig. 4(a)). This association with low heating power suggests the neoclassical Ware pinch for which $\Gamma_W \approx \varepsilon^{1/2} n E_T / B_P \sim n/T^{3/2}$. For the discharge shown in Fig. 1 at 3500 ms Γ_W ($\rho = 0.3$) $\approx 0.09 \times 10^{20}$ m^{-2} s^{-1}. A transport analysis of this discharge gives $\chi_{EFF} = (q_e + q_i)/(n_e \nabla T_e + n_i \nabla T_i) \approx 0.5$ m^2 s^{-1}. Taking $D \sim \chi_{EFF}/4$ (this is roughly equivalent to $\tau_P = \tau_E$ since $L_T/L_n \approx 4$), the diffusive particle flux $\Gamma_D \approx 0.19 \times 10^{20}$ m^{-2} s^{-1} would be comparable to the Ware pinch flux. Making the simple estimate that the core confinement scales like the global confinement, or roughly $\tau_E^{Core} \propto I_P/P^{0.5}$, then $D \sim \chi \propto nTL_T/I_P^2$, where L_T is the temperature gradient scale length, which is invariant for stiff profiles. The condition at which the Ware pinch would balance the diffusive particle flux is given by $D\nabla n \sim nT\nabla n/I_P^2 \sim \Gamma_W \sim n/T^{3/2}$, or $\nabla n/n_G \propto I_P/T^{5/2}$ which is

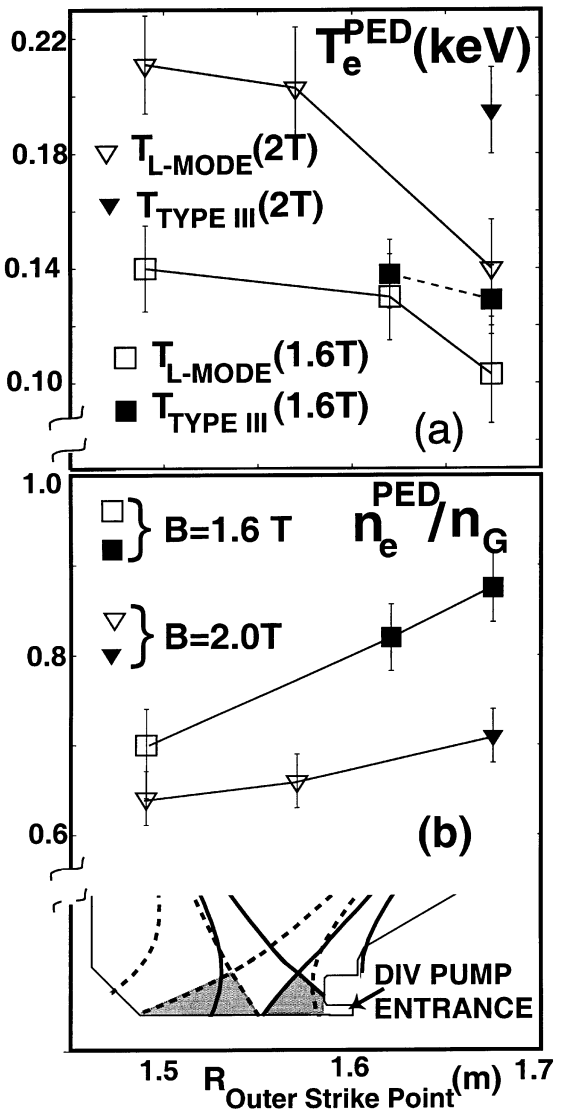

Fig. 3. (a) The critical temperature for transition to Type III ELMs (filled points) and L-mode (open points) as a function of the divertor strike point radius for $I_P = 1.2$ MA. At small R_{DS} transition is directly from Type I to L-mode, while at large R_{DS} transition is first to Type III ELMs. (b) Data for two different toroidal fields are shown. (c) Result of variation of transition temperatures is that pedestal density obtainable with Type I ELMs (good confinement) increases with R_{DS} as a composite of Type III and L-mode thresholds; insert shows range of R_{DS}.

consistent with the data for the high density discharges. A transport analysis assuming $D \sim \chi_{EFF}/4$ also indicates that the Ware pinch may be of sufficient size near the magnetic axis to account for the density profile peaking although the overall profile evolution is not matched.

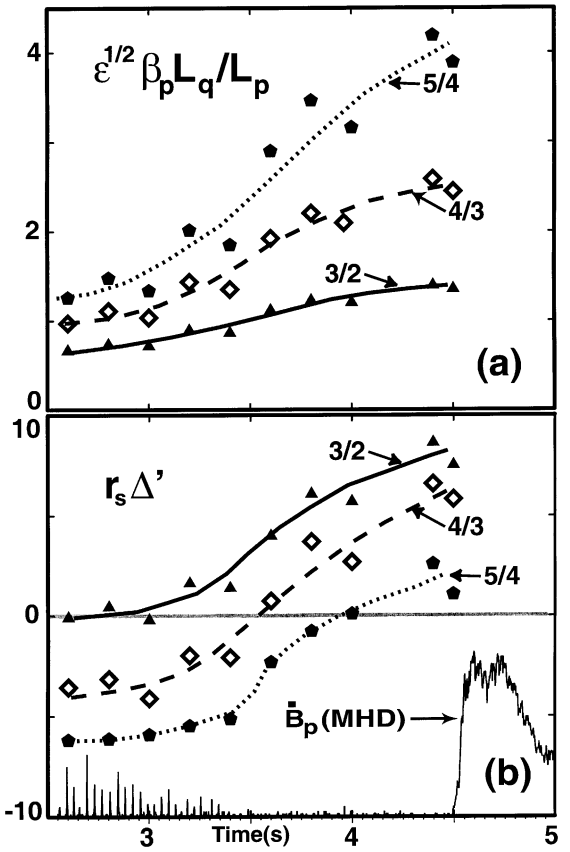

Fig. 4. Termination of high density phase for discharge of Fig. 1. (a) The neoclassical drive term increases with time due to peaking of the pressure profile. Higher order modes closer to the magnetic axis show the strongest rise since pressure peaking is strongest on axis and average poloidal field decreases near axis (β_p term). (b) Classical tearing mode drive term is also increasing with time due to peaking of current density profile (through bootstrap current associated with the pressure peaking).

5. Termination event

The density and stored energy rise in discharges that reach densities $>1.1 \times n_G$ is terminated by the onset of MHD modes (Fig. 1). Typically a series of modes with poloidal mode number, m, over toroidal mode number, $n, = 3/2, 4/3, 5/4, \ldots$ in the region just outside the $q = 1$ surface are observed. The higher n modes were usually observed first, while strong confinement loss was associated with the 3/2 mode. This region, $\rho = 0.3$–0.6, has increasing pressure gradient as a result of the peaking of the density profile. The tearing mode island growth is roughly described by $d\hat{w}/d\hat{t} \approx \Delta' r_S + \varepsilon^{1/2}\beta_P(L_q/L_P)(1 - g\rho_\theta^2/w^2)/\hat{w} - c\hat{w}$ [12]. Here $\hat{w}$ is the island width, w, normalized to the minor radius of the singular surface, r_S. $\hat{t}$ is time normalized to the resistive time, and β_P the

poloidal β where these parameters apply to the region within r_S. L_q and L_P are the scale lengths for the q and pressure profiles; ρ_θ is ion poloidal gyro radius (g and c are constants which may depend on collisionality); and ε is the inverse aspect ratio, where these quantities are evaluated at r_S. The second term is the neoclassical drive that becomes strong when the island width exceeds ρ_θ. The multiplier on this term, $\varepsilon^{1/2}\beta_P(L_q/L_P)$, increases in time as a consequence of the pressure profile peaking particularly for the higher n modes (Fig. 4(a)) which see the highest pressure gradient increase and largest pressure increase relative to the average enclosed poloidal field. As a consequence of the peaking of the density and pressure profiles, the bootstrap current peak moves radially inward and increases in magnitude. This increases the current density gradient and thus the classical tearing mode drive $\Delta' r_S$ (Fig. 4(b)). Δ' is calculated using the PEST3 code [13]. The Δ' calculation is very sensitive to details of the current density profile and it is likely the trend with time is more accurate than the absolute value. Since the neoclassical drive does not apply below a critical seed island width, the sudden growth of the modes suggests that neoclassical terms are important, as does the appearance of the higher n modes first.

6. Summary and conclusions

Discharges on DIII-D demonstrate that it is possible to exceed the Greenwald density while maintaining good energy confinement and reasonable β_N. The consequence of this result for Tokamak reactors however is unclear. If the density peaking is a result of the Ware pinch, the scaling of this effect to a large device is unfavorable. Alternately however, a pinch effect can result in the context of turbulent transport under the conditions where the electron bounce frequency is high compared to the mode frequency [14]. This results in a density profile consistency that may be expected to produce similar profiles in large devices. The possible connection between edge resistivity and reduction in the edge pressure at high density is favorable for large tokamaks that are expected to have much higher H-mode pedestal temperatures (based on the present understanding of the scaling of the H-mode pedestal width and critical edge pressure gradient [15]). Finally the large leverage the pedestal pressure has over the global confinement may be relaxed at higher temperature where the temperature profiles transition from stiff, with constant gradient scale length, to additive, with pedestal temperature at constant gradient [16].

The increase in H–L transition temperature with increased triangularity of the x-point may be a simple consequence of the increased toroidal field at reduced major radius [8]. It is also possible that the geometry of the x-point region may effect the ion orbit loss.

It may be possible to avoid the neoclassical tearing mode that terminates the high density discharges using the high electron cyclotron heating power now available on DIII-D. ECH current drive might be used to flatten the current profile in the neighborhood of the $q = 1.5$ surface to reduce the size of the seed island, or direct heating of the mode has also been shown to stabilize NTMs [17]. It may also be possible to avoid these modes by reversing the magnetic shear (the sign of L_q) since this eliminates the neoclassical drive.

References

[1] ITER Physics Basis Editors et al., Nucl. Fus. 39 (1999) 2137.
[2] ITER Physics Expert Groups on Confinement and Transport and Confinement Modeling and Database et al., Nucl. Fus. 39 (1999) 2175.
[3] V. Mertens, in: Proceedings of the 16th International Conference on Plasma Physics and Controlled Nuclear Fusion Research, vol. 1, Montreal, Canada, 1996, p. 413.
[4] D.J. Campbell et al., Plasma Phys. Control. Fus. 38 (1996) 1497.
[5] H. Zohm, Plasma Phys Control. Fus. 38 (1996) 105.
[6] O. Pogutse et al., Proceedings of the 24th EPS Conference on Controlled Fusion and Plasma Physics, vol. 21A, Berchtesgaden, Germany, 1997, p. 1041.
[7] O. Pogutse et al., Proceedings of the 26th EPS Conference on Controlled Fusion and Plasma Physics, vol. 23J, Maastricht, Netherlands, 1999, p. 249.
[8] A.E. Hubbard, Proceedings of the 16th International Conference on Plasma Physics and Controlled Nuclear Fusion Research, vol. 1, Montreal, Canada, 1996, p. 875.
[9] W. Suttrop, Plasma Phys. Control. Fus. 39 (1997) 2051.
[10] T.H. Osborne et al., Plasma Phys. Control. Fusion 42 (2000) A175.
[11] J.R. Ferron et al., Phys. Plasmas 7 (2000) 1976.
[12] H.R. Wilson et al., Phys. Plasmas 3 (1996) 248.
[13] A. Pletzer, J. Comput. Phys. 115 (1994) 530.
[14] D.R. Baker et al., Phys. Plasmas 5 (1998) 2936.
[15] M. Sugihara et al., Proceedings of the 26th EPS Conference on Controlled Fusion and Plasma Physics, vol. 23J, Maastricht, Netherlands, 1999, p. 1449.
[16] J. Janeschitz et al., Proceedings of the EPS Conference on Controlled Fusion and Plasma Physics, vol. 23J, Maastricht, Netherlands, 1999, p. 1445.
[17] H. Zohm et al., Proceedings of the EPS Conference on Controlled Fusion and Plasma Physics, vol. 23J, Maastricht, Netherlands, 1999, p. 1373.